The Fifth International Symposium on Computational Wind Engineering (CWE2010)
Chapel Hill, North Carolina, USA May 23-27, 2010

Numerical study on flow fields of tornado-like vortices using the LES turbulence model

Takeshi Ishihara[a], Sho Oh [b], Yoshiteru Tokuyama [c]

[a],*Department of Civil Engineering , School of Engineering, The University of Tokyo, 7-3-1, Hongo ,Bunkyo-ku, Tokyo, Japan, ishihara@bridge.t.u-tokyo.ac.jp*
[b] *Department of Civil Engineering , School of Engineering, The University of Tokyo, 7-3-1, Hongo ,Bunkyo-ku, Tokyo, Japan, s.oh@bridge.t.u-tokyo.ac.jp*
[c] *M&T Co., LTD, Art Center of Tokyo Bld. 11F, 1-4-1, Senju, Adachi-ku, Tokyo , Japan, yoshiteru.tokuyama@jpmandt.com*

ABSTRACT: Flow fields of tornado-like vortices generated by a numerical tornado simulator have been investigated using the LES turbulence model for two typical swirl ratios. The results showed that the core radii of vortices with swirl ratios of 0.31 and 0.65 agree favorably with visualized vortices by a laboratory tornado simulator. Mean velocity fields were examined to obtain detailed corner flow patterns. It was found that a one-cell type vortex with a central upward flow appears for the case of low swirl ratio and vertical velocities show peaks at the center of the vortex, while a two-cell type vortex with a central downward flow emerges for the case of high swirl ratio and the maximum tangential velocity appears near ground. The formations of one-cell and two-cell type vortices were investigated by examining axisymetric time averaged Navier-Stokes equations. The vertical pressure gradient generates vertical velocities at the center of vortex in the one-cell type vortex, while the centrifugal force balances with the radial pressure gradient and the vertical advection term of the radial velocity in the two-cell type vortex.

1 INTRODUCTION

Tornados are vortices with strong three-dimensional flow fields and cause damages more serious than other wind-induced disasters. Wind resistant design against tornados requires accurate information about the three-dimensional flow field of tornado. However, little information could be acquired by field measurements due to its small spatial scale and low frequency of occurrence. Laboratory experiments have been conducted by Ward (1972), Wan and Chan (1972) Monji and Mitsuta (1984), Matsui and Tamura (2006) and Haan et al. (2008) in order to obtain the detailed information of the flow field of tornado-like vortex. Numerical simulations have also been conducted by Howells et al. (1988), Lewellen and Lewellen (1997, 2007), Lewellen et al.(1999) and Kuai et al. (2008). The mechanism of the formation of three-dimensional flow fields in tornado-like vortices has not been fully proven yet.

This paper presents some results obtained by a numerical tornado simulator using LES turbulence model. Section 2 describes the numerical model used in this study. In Section 3, the three-dimensional flow fields are examined and compared with the experimental data to verify the performance of the numerical model. Finally axisymetric time averaged Navier-Stokes equations are evaluated to reveal the mechanism of the formation of the flow field in section 4.

2 NUMERICAL MODEL

2.1 *Governing equations and turbulence model*

The governing equations employed in LES model are obtained by filtering the time-dependent Navier-Stokes equations as follows:

$$\frac{\partial \rho \tilde{u}_i}{\partial x_i} = 0 \tag{1}$$

$$\frac{\partial}{\partial t}(\rho \tilde{u}_i) + \frac{\partial}{\partial x_j}(\rho \tilde{u}_i \tilde{u}_j) = \frac{\partial}{\partial x_j}\left(\mu \frac{\partial \tilde{u}_i}{\partial x_j}\right) - \frac{\partial \tilde{P}}{\partial x_i} - \frac{\partial \tau_{ij}}{\partial x_j} \tag{2}$$

where $\tilde{u}_i$ and $\tilde{p}$ are filtered mean velocity and filtered pressure respectively. ρ is density, τ_{ij} is subgrid- scale stress and is modeled as follows:

$$\tau_{ij} = -2\mu_t \tilde{S}_{ij} + \frac{1}{3}\tau_{kk}\delta_{ij} \quad , \qquad \tilde{S}_{ij} \equiv \frac{1}{2}\left(\frac{\partial \tilde{u}_i}{\partial x_j} + \frac{\partial \tilde{u}_j}{\partial x_i}\right) \tag{3}$$

where μ_t is subgrid-scale turbulent viscosity, and $\tilde{S}_{ij}$ is the rate-of-strain tensor for the resolved scale.

Smagorinsky-Lilly model is used for the subgrid-scale turbulent viscosity,

$$\mu_t = \rho L_s^2 \left|\tilde{S}\right| = \rho L_s \sqrt{2\tilde{S}_{ij}\tilde{S}_{ij}} \quad , \qquad L_s = \min\left(\kappa\delta, C_s V^{1/3}\right) \tag{4}$$

where L_s is the mixing length for subgrid-scales, κ is the von Karman constant, 0.42, C_s is Smagorinsky constant, δ is the distance to the closest wall and V is the volume of a computational cell. In this study, C_s is determined as 0.032 as used in Oka and Ishihara (2009).

Finite volume method and unstructured collocated mesh are used for the present simulations. SIMPLE (semi-implicit pressure linked equations) algorithm is employed for solving the discritized equations (Ferziger and Peric, 2002)

2.2 *Configurations of the numerical tornado simulator*

In this study, Ward-type tornado simulator is numerically modeled. Figure 1 shows the overview of the numerical tornado simulator and mesh used in the simulation. Mesh density is higher at center to capture the vortex structure. Constant velocity boundary condition is given at the top of the simulator to generate upward flow in the tornado.

Swirl ratio is an important parameter to determine the structure of a tornado-like vortex. The swirl ratio defined by Ward (1972) is used in this study as follows:

$$S = S_E = \frac{\tan\theta}{2a} \tag{5}$$

where θ is the angle of the guide vane, and a is the aspect ratio of the inflow height , h, to the radius of the hole , r_0.

Two representative swirl ratios are chosen to examine the different type of the structure of vortex. The case of $S = 0.31$ represses a low swirl ratio vertex and the case of $S = 0.65$ denotes a high swirl ratio one. Table1 shows the parameters used in this study, where V_c is the maximum tangential velocity at the radius of r_c in a cyclostrophic balance region.

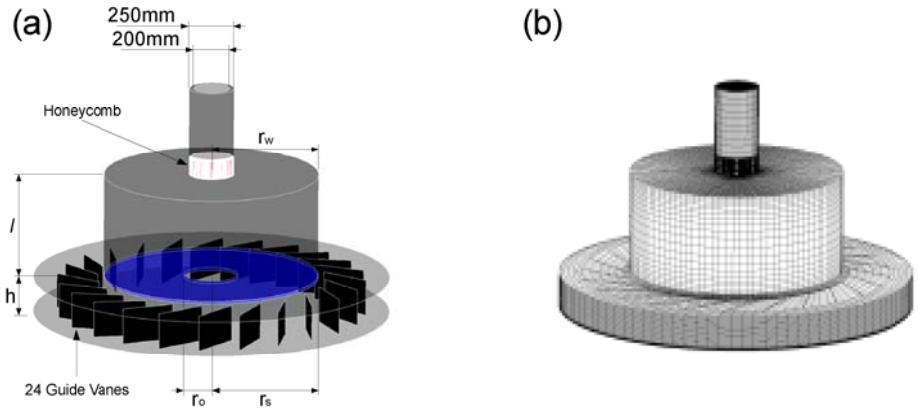

Figure1. (a) Overview of the numerical tornado simulator and (b) mesh used in this study.

Table 1. Parameters and representative values used in this study.

Case	a	θ	S	V_c	r_c
1	1.33	40deg.	0.31	13.0m/s	4.83mm
2	1.33	60deg.	0.65	8.3m/s	32.5mm

3 MEAN VELOCITY AND PRESSURE FIELD

In order to examine flow field in the tornado-like vortices, the simulated vortices are visualized by the instantaneous streamlines and compared with the flow visualization obtained from the experiment. The normalized mean velocities as well as pressures are discussed and compared with the laboratory data in this section.

Experimental results obtained by Monji and Mitsuta(1984) and Matsui and Tamura (2006) are used for the validation of the numerical model. Monji and Mitsuta measured the vertical velocity using hot-wire anemometer, while Matsui and Tamura measured the tangential velocity using the laser Doppler velocimeter.

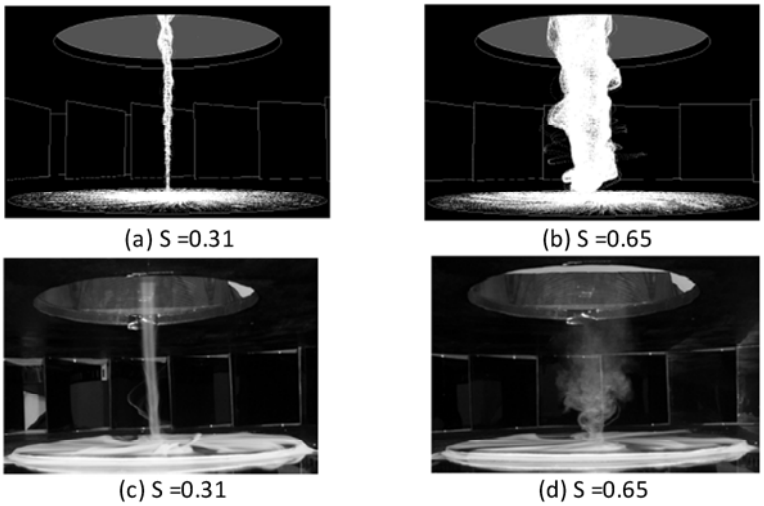

Figure 2. Comparison of (a, b) streamlines calculated by the numerical simulation and (c, d) flow visualizations.

Comparisons of the instantaneous streamlines calculated from the numerical results and the flow visualizations obtained from the laboratory by Matsui and Tamura (2006) are shown in Figure.2. Streamlines and flow visualizations show that the core radii are small for the low swirl ratio case and large for the high swirl ratio one. The shapes of the vortices show satisfactory resemblance, indicating that the numerical simulator can generate tornado-like vortex as the laboratory simulator.

The flow patterns strongly depend on the swirl ratio. The predicted velocity vectors in $r-z$ plane are shown in Figure 3 for the two swirl ratios, where z is the height and r is the radius. In the Figure 3(a), a strong updraft appears in the center of the vortex, forming a one-cell type vortex for the case of $S=0.31$, while a downward flow reveals in the center of the vortex generating a two-cell type vortex for the case of S=0.65 in Figure 3(b). In order to examine mean velocities in the vortices, radial distribution of normalized velocity components are plotted at various heights in Figure 4 to 6 for the two swirl ratios.

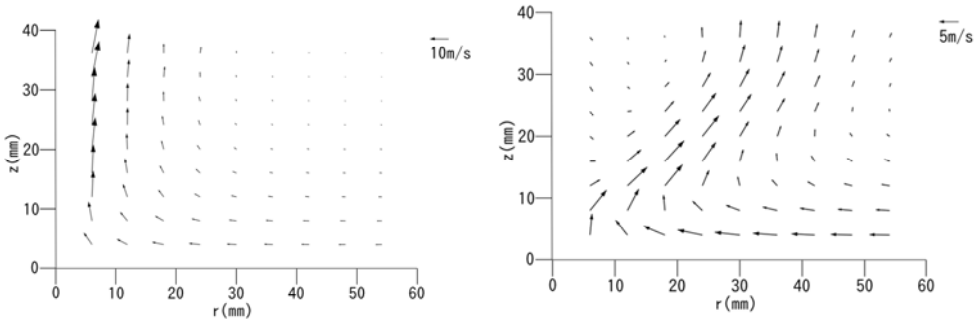

(a) $S=0.31$ (b) $S=0.65$

Figure 3. Velocity vectors in r-z plane for (a) $S=0.31$ and (b) $S=0.65$.

In the case of $S=0.31$, the mean radial velocities are all negative and decreases with the increase of height as shown in Figure 4(a). The maximum value appears at the lowest elevation of $z=0.2r_c$ and reaches to $0.5V_c$. On the other hand, the mean radial velocities in the case of $S=0.65$ show positive values near the center of the vortex at the lower elevations. The absolute values of maximum positive and negative radial velocities are close to $0.5V_c$. The maximum normalized radial velocities in these two cases are same as the value proposed by Simiu and Scanlan (1996).

Figure 5 shows radial distributions of normalized tangential velocity at various heights obtained from the numerical simulations and experiment by Matsui and Tamura (2006). Velocity distributions at two higher elevations are almost the same, and predicted tangential velocities agree satisfactorily with laboratory data. In the surface layer, tangential velocities decrease in the case of $S=0.31$, while they increase in the case of $S=0.65$. The maximum value for $S=0.65$ reaches to $1.4V_c$. This increase in the tangential velocity near the surface is important for wind resistant design, since most of engineering structures exist in this region.

Radial distributions of normalized vertical velocities at various heights for two swirl ratios are shown in Figure 6. In the case of $S=0.31$, the vertical velocities take their maximum values at the center of the vortex and increase with the increase of height. The maximum vertical velocity is about $1.8V_c$ at $z=2r_c$. On the other hand, for $S=0.65$, the vertical velocities show their maximum values close to $0.6V_c$, which are almost same as the value of $0.67V_c$ proposed by Simiu and Scanlan (1996). The normalized vertical velocities

from the laboratory by Mitsuta and Monji (1984) are also plotted in Figure 6 (b) for the comparison and the predicted velocities at $z = 2r_c$ show a good agreement with the measured those at $z = 1.3r_c$.

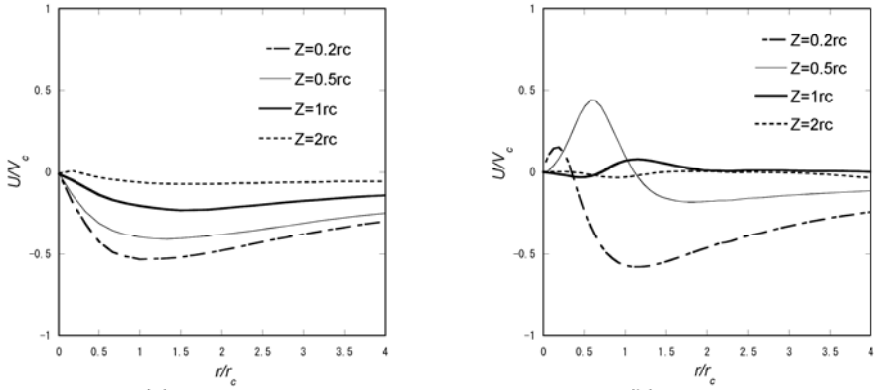

Figure 4. Radial distribution of normalized radial velocities at various heights for (a) $S = 0.31$ and (b) $S = 0.65$.

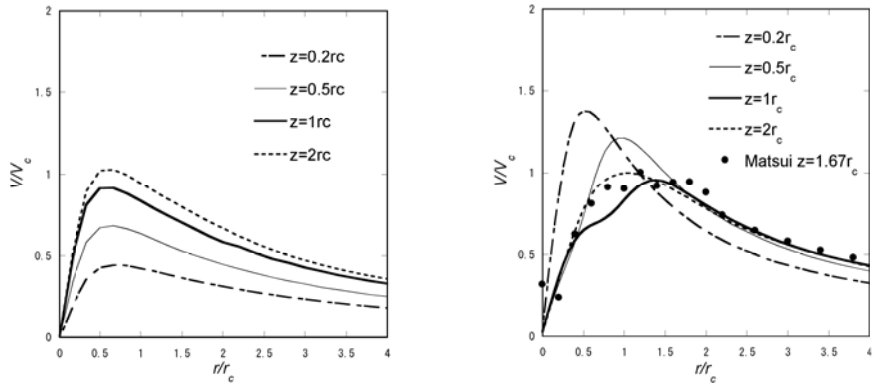

Figure 5. Radial distribution of normalized tangential velocities at various heights for (a) $S = 0.31$ and (b) $S = 0.65$. Matsui denotes laboratory data obtained by Matsui and Tamura (2006).

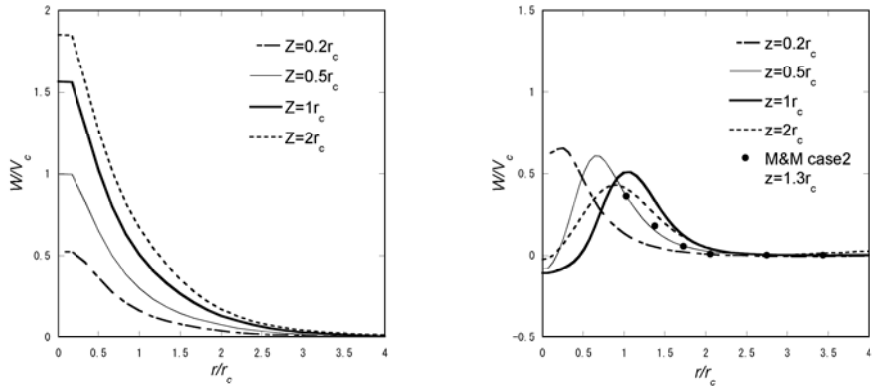

Figure 6 Radial distribution of normalized vertical velocities at various heights for (a) $S = 0.31$ and (b) $S = 0.65$. M&M denotes laboratory data obtained by Monji and Mitsuta (1984).

Figure 7 shows radial distribution of normalized pressure at various heights for $S = 0.31$ and $S = 0.65$. It is obvious that there are distinct differences between these two cases. In the case of $S = 0.31$, pressure gradients decreases rapidly with the increase of height, while pressure gradient at various heights are almost same in the case of $S = 0.65$.

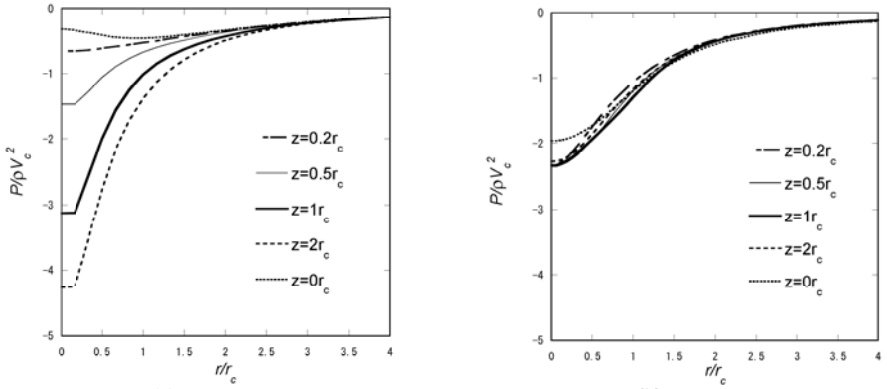

Figure 7. Radial distribution of normalized pressure at various heights for (a) $S = 0.31$ and (b) $S = 0.65$

4 FORCE BALANCES IN THE TORNADO-LIKE VORTICES

Considering the tornado induced damages to the structures, the high wind speeds observed in the numerical tornado simulator are important and their mechanisms have to be revealed. In this section, axisymmetric time-average Navier-Stokes equations are derived and the force balances are investigated to reveal the mechanism of those phenomena.

To examine the mechanism of the high vertical velocity at the center of the vortex in the case of $S = 0.31$, vertical components of the axisymetrical Navier-Stokes equation is derived as:

$$U\frac{\partial W}{\partial r} + W\frac{\partial W}{\partial z} = -\frac{1}{\rho}\frac{\partial P}{\partial z} - \left(\frac{\partial uw}{\partial r} + \frac{\partial w^2}{\partial z} + \frac{uw}{r}\right) + D_w \tag{6}$$

where u, v and w denote the radial, tangential and vertical component of fluctuating velocity, z is the height above ground and r is the radius from the center of the simulator.

The left hand side consists of radial (A_{rw}) and vertical (A_{zw}) advection terms. The right hand side of the equation is the vertical pressure gradient term (P_z), Reynolds stress term (T_w), and the diffusion term (D_w). For the low swirl ratio case, four terms in Eq. (6) on the vortex axis are estimated and shown in Figure 8 (a). Among all the terms, the contributions from the vertical pressure gradient and the vertical advection term are dominant. This indicates that this equation can be approximated as the balance equation of vertical pressure gradient and the vertical advection. From this balance, the vertical wind velocity, W, can be predicted as:

$$W = \sqrt{2\int\left(-\frac{1}{\rho}\frac{\partial P}{\partial z}\right)dz} \tag{7}$$

The estimated vertical velocity from the pressure gradient by this model and the simulated vertical velocity are shown in Figure 8 (b). The proposed model shows good agreement with the simulation, which suggests the large vertical velocity in case of S=0.31 is formed by the large pressure gradients.

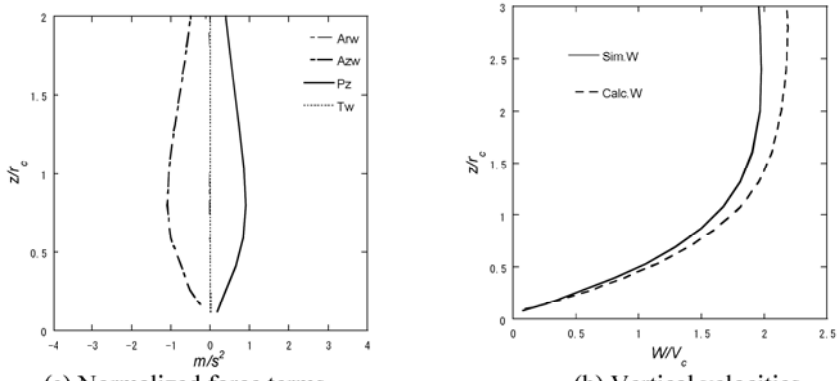

(a) Normalized force terms (b) Vertical velocities

Figure 8 Vertical distribution of (a) normalized force terms of Navier-Stokes equation and (b) the vertical velocities at $r = 0$ for $S = 0.31$.

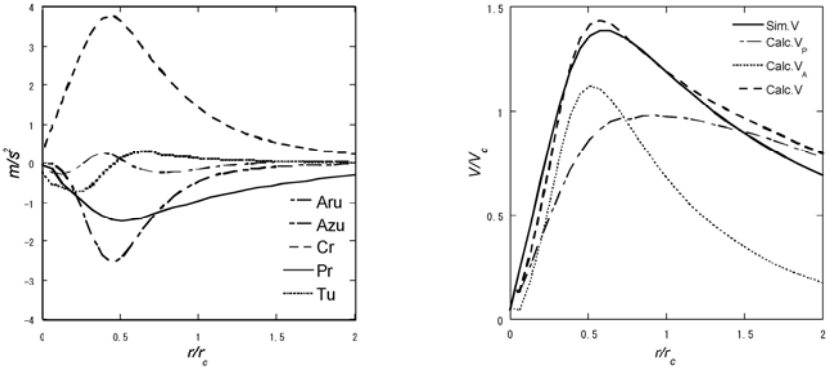

(a) Normalized force terms (b) Tangential velocities

Figure 9. Radial distribution of (a) normalized force terms of Navier-Stokes equation and (b) the tangential velocities at $z = 0.25r_c$ for $S = 0.65$.

The mechanism of the strong tangential velocity in the high swirl ratio case is investigated by considering the force balance of the radial component of the Navier-Stokes equation. The radial term of the axisymetric Navier-Stokes equation can be written as:

$$U\frac{\partial U}{\partial r}+W\frac{\partial U}{\partial z}-\frac{V^2}{r}=-\frac{1}{\rho}\frac{\partial P}{\partial r}-\left(\frac{\partial u^2}{\partial r}+\frac{\partial uw}{\partial z}-\frac{v^2}{r}+\frac{u^2}{r}\right)+D_u \tag{8}$$

The left hand side of this equation consists of the radial (A_{ru}) and vertical (A_{zu}) advection term and the centrifugal force term (C_r). The right hand side of the equation is the radial pressure gradient term (P_r), Reynolds stress term (T_u), and the diffusion term (D_u). Five terms in Eq. (8) at the heights of $z = 0.25r_c$ and $z = 3.0r_c$ are estimated and those at $z = 0.25r_c$ are shown in Figure 9 (a) for the high swirl ratio case. The centrifugal force at $z = 3.0r_c$ balances with the pressure gradient term, while that at $z = 0.25r_c$ balances with the pressure gradient term and the vertical advection term, and the tangential velocity, V, can be estimated as:

$$V=\sqrt{V_p^2+V_A^2}=\sqrt{\frac{1}{\rho}\frac{\partial P}{\partial r}r+W\frac{\partial U}{\partial z}r} \tag{9}$$

The tangential velocities calculated by this model and those from the simulation are plotted in Figure9 (b). The calculated tangential velocity by the model shows good agreement with the simulation. The tangential velocity, V_p, is smaller than the simulated one when the tangential velocity is estimated by the pressure gradient term. This indicates that the increase of tangential velocity near the surface in the two-cell type vortex comes from

the vertical advection term (A_{zu}). The mechanism of the flow field is supposed that pressure gradient is independent of the height and the ground pressure gradient does not balance with the centrifugal force because of the friction. As a result, large radial inflow occurs near the ground and causes the increase in the tangential velocity there.

5 CONCLUSION

In this study, flow fields of tornado-like vortices generated by a numerical tornado simulator have been investigated using the LES turbulence model for two typical swirl ratios. Following conclusions were obtained.

1) The core radii of vortices with swirl ratios of 0.31 and 0.65 from the numerical tornado simulator agree favorably with visualized vortices by the laboratory one.
2) A one-cell type vortex appears for the low swirl ratio case, in which the vertical velocities show peaks at the center and the tangential velocity decreases as the height decreases. On the other hand, a two-cell type vortex appears for the high swirl ratio case, in which the maximum tangential velocity appears at the level close to the ground and the peaks of vertical velocity are observed near the radius of maximum tangential wind.
3) The maximum vertical velocity at the center of the vortex is generated by the vertical pressure gradient and reaches 1.8 times of V_c for the low swirl ratio case. On the other hand, the centrifugal force at the height of $z = 0.25r_c$ balances with the radial pressure gradient and the vertical advection term of the radial velocity, and the maximum tangential velocities there is as much as 1.4 times of V_c for the high swirl ratio case.

6 REFERENCES

Ferziger, J., Peric, M, 2002. Computational method for fluid dynamics, 3rd Edition, Springer.
Haan, F.L., Sarkar, P.P., Gallus, W.A., 2008. Design, construction and performance of a large tornado simulator for wind engineering applications, Engineering Structures 30, 1146-1159.
Howells, P.C., Rotunno, R., Smith, R.R., 1988. A comparative study of atmospheric and laboratory analogue numerical tornado-vortex models. Quarterly Journal of Royal Meteorological Society, 114 , 801-822.
Kuai, L., Haan, F.L., Gallus, W.A., Sarkar, P.P., 2008. CFD simulations of the flow field of a laboratory simulated tornado for parameter sensitivity studies and comparison with field measurements, Wind and Structures, Vol.11, No.2, 1-22.
Lewellen, D.C., Lewellen, W.S., 1997. Large-eddy simulation of a tornado's interaction with the surface. Journal of the Atmospheric Sciences, Vol.54, No.5, 581-605.
Lewellen, D.C., Lewellen, W.S., Xia, J., 1999. The influence of a local swirl ratio on tornado intensification near the surface. Journal of the Atmospheric Sciences, Vol.57, 527-544.
Lewellen, D.C., Lewellen, W.S., 2007. Near-surface intensification of tornado vortices. Journal of the Atmospheric Sciences, Vol.64, 2176-2194.
Matsui, M., Tamura, Y., 2006. Experimental study on tornado-like flow as functions of swirl ratio and surface roughness, Proc. of the 19th National Symposium on Wind Engineering, 7-12 (In Japanese).
Mitsuta,Y., and Monji, N., 1984. Development of a laboratory simulator for small scale atmospheric vortices, Natural Disaster Science,Vol.6, 43-54.
Nolan, D.S., Purcell, O.P., 1999. The structure and dynamics of tornado-like vortices. Journal of the Atmospheric Sciences, Vol.56, 2908-2936.
Oka, S. and Ishihara, T., 2009. Numerical study of aerodynamic characteristics of a square prism in a uniform flow, *J. Wind Eng. Indust. Aerodyn.*, Vol. 97, pp.548-559.
Simiu,E. and Scanlan R.N.,1996 Wind effects on structures : fundamental and applications to design, 3rd Edition, John Wiley & Sons.
Wan, C.A., Chang, C.C., 1972. Measurement of the velocity field in a simulated tornado-like vortex using a three-dimentional velocity probe, Journal of Atmospheric Science,Vol.29, 116-127.
Ward, N.B., 1972. The exploration of certain features of tornado dynamics using a laboratory model, Journal of the Atmospheric Sciences, Vol.29, 1194-1204.